1
2 **Authors' response to referees**
3
4 We thank both referees for their supporting comments and good suggestions to
5 improve our manuscript.
6 During the revision, we recognized a mistake in the conversion of TEP fluxes
7 reported by Martin et al (2011) and Ebersbach et al (2014) into TEP-C fluxes. We
8 corrected this mistake. The change did not affect our interpretations.
9
10 <u>Anonymous Referee #1</u>
11 Received and published: 15 December 2016
12 Review of bg-2016-508 Particle export fluxes to the oxygen minimum zone of the
13 Eastern
14 Tropical North Atlantic Anja Engel, Hannes Wagner, Frédéric A. C. Le Moigne,
15 Samual T. Wilson
16 The authors present a study of vertical fluxes collected with surface tethered drifting
17 sediment trap from the Eastern Tropical North Atlantic. They collected settling
18 material
19 from 7 depths; 60 m, 100 m, 150 m, 200 m, 300 m, 400 m, 500 m, and 600 m. Depth
20 between 300 and 500 m were sampling within the oxygen minimum zone. The main
21 findings in the study was that transfer efficiencies in an oxygen minimum zone were
22 higher than expected when only considering temperature dependency for the
23 microbial
24 degradation of organic matter and that the composition of the organic matter within
25 the settling aggregates had a large impact on the transfer efficiencies. The latter
26 finding
27 was evident through observations of higher attenuation of amino acids comparedto
28 polysaccharide-rich TEP. The manuscript is well written and the date clearly
29 presented.
30 I only have some minor issues regarding the vertical flux of TEP (see specific
31 comments). I recommend the manuscript for publication in Biogeosciences with
32 minor
33 revision.Specific comments:
34
35 Line 57: Please insert a comma after ".. (Volk and Hoffert, 1985)".
36
37 *Response: comma was inserted*
38
39 Line 210: Were the filters for the elemental analyzer wrapped in tin foil or packed in
40 aluminium cups?
41
42 *Response: The filters were enclosed in tin cups; information was added.*
43
44 Line 364: The Gum Xanthan flux is per square meter, please correct to m-2 d-1 for
45 both Martin et al. (2011) and Ebersbach et al. (2014).
46
47 *Response: Units were corrected*
48
49 Line 388-389: It could also be due to slower sinking velocities. It is not possible to
50 say from b alone which process is driving the values. However, you can say that
51 more

52 degradation occurred within a depth region, either due to faster degradation or slower
53 settling.
54
55 *Response: Potential effect of reduced sinking velocity was included*
56
57 Line 417-419: Looking at figure 3c, I do not see this trend? For deployment #2 there
58 is
59 an increase above the OMZ, then a slight decrease between 200 and 300 m
60 whereafter
61 it is stable and then show a decrease between 500 and 600 m. For deployment #1 it
62 seems like there is no significant changes in TEP flux between 150 and 600 m. So I
63 do not see that there is a clear different between TEP fluxes within the OMZ
64 compared
65 to below.
66
67 *Response: During both deployments no clear decrease in TEP fluxes was*
68 *determined for the OMZ. TEP fluxes decreased between 500 and 600m, i.e. below*
69 *the OMZ; this was more pronounced during the second deployment. We will modify*
70 *the text to clarify this better.*
71
72 Line 464-466: This was only observed for deployment #2, not for deployment #1.
73 Deployment#1 showed decreasing ratios already within the OMZ, 400 to 500 m.
74
75 *Response: Correct, we will modify the text to state that a decrease in TEP-C:POC*
76 *ratios below the OMZ was only observed during deployment #2.*
77
78
79
80 **Anonymous Referee #2**
81 Received and published: 10 February 2017
82 **Particle export fluxes to the oxygen minimum zone of the Eastern Tropical**
83 **North**
84 **Atlantic**
85 This paper by Engel et al. describes the flux and composition of particles from
86 surface
87 waters through the oxygen minimum zone of the water column off the coast of
88 Mauritania
89 in the Eastern Tropical North Atlantic. Two deployments of surface-tethered drifting
90 sediment traps collected particles at 7-8 depths including the OMZ from 300-500m.
91 Calculated transfer efficiencies of the total POM and various characterized
92 components
93 of the particles indicate lower attenuation through the OMZ than predicted from
94 seawater temperature. Particle composition data showed highest transfer efficiencies
95 for TEP and lowest for amino acids. The paper is well written and a nice contribution
96 regarding particle flux dynamics in OMZs. I have no major issues with the text and
97 recommend publication after minor revisions detailed below.
98
99 **Minor comments:**
100 - pg 3, line 57: add comma after citation
101 - pg 4, line 81: ref LeMoigne et al., 2012 is missing from reference list; LeMoigne et
102 al., 2016 is listed but not cited, perhaps one of these is an error

103 - pg 4, line 85: typo, Alldredge is misspelled
104 - pg 4, line 98: typo, change 'be' to 'been'
105 - pg 5, line 130 (and elsewhere throughout): I am not familiar with this spelling of
106 'Mauretania' with an e and could not find other references to Mauritania spelling as
107 such so would recommend changing (certainly if this is an accepted spelling it does
108 not need to be changed)
109 - pg 5, line 131: 'drifting' is written twice
110 - pg 6, line 145: hyphenate 'surface-tethered'
111 - pg 8, line 185: insert 'of' (Aliquots of samples: : :)
112 - pg 9, line 215: remove 'in' (: : :were filtered onto: : :)
113 - pg 9, line 221: hyphenate 'peroxydisulphate-containing'
114 - pg 9, line 231: ref Dittmar et al., 2009 is missing from reference list
115 - pg 11, line 269: close parentheses after 'sample'
116 - pg 17, line 432: opal is incorrectly capitalized
117 - pg 19, line 488: Keil et al., 2016 is missing from reference list (or incorrectly cited
118 here as 2015 is in the list)
119 - pg 20, line 494: insert 'the' (: : :explain the relative: : :)
120 - pg 24, lines 592-600: the two Buesseler et al., 2007 references should be
121 distinguished
122 as a and b here and when cited in the manuscript
123 - pg 26, line 652: Giering reference is formatted incorrectly (begins with 'Sarah')
124 - pg 27, line 675: Kartensen et al., 2008 is not cited in manuscript but is listed here
125 - pg 31, line 760: Ploug and Jorgensen, 1999 is not cited in manuscript but is listed
126 here
127 - pg 34: If possible, it would be nice to include the calculated degradation indices
128 along
129 with the amino acid composition in table 2.
130
131
132 *Response: All suggestions have been considered. Values for the DI's have been*
133 *included in table 2.*
134

135

136

137

138

Particle export fluxes to the oxygen minimum zone of the

Eastern Tropical North Atlantic

141

142

143

Anja Engel[1], Hannes Wagner[1], Frédéric A. C. Le Moigne[1], Samuel T. Wilson[2]

145

[1] GEOMAR Helmholtz Centre for Ocean Research Kiel,
24105 Kiel, Germany

[2] Daniel K. Inouye Center for Microbial Oceanography: Research and Education, Department
of Oceanography, University of Hawaii, Honolulu, HI 96822, USA

Correspondence to: Anja Engel (aengel@geomar.de)

155
156

157

158

159

160

161

Abstract. In the ocean, sinking of particulate organic matter (POM) drives carbon export from the euphotic zone and supplies nutrition to mesopelagic communities, the feeding and degradation activities of which in turn lead to export flux attenuation. Oxygen (O_2) minimum zones (OMZs) with suboxic water layers (<5 µmol O_2 kg^{-1}) show a lower carbon flux attenuation compared to well oxygenated waters (>100 µmol O_2 kg^{-1}), supposedly due to reduced heterotrophic activity. This study focuses on sinking particle fluxes through hypoxic mesopelagic waters ($<60\%$ µmol O_2 kg^{-1}); these represent ~100 times more ocean volume globally compared to suboxic waters, but have less been studied. Particle export fluxes and attenuation coefficients were determined in the Eastern Tropical North Atlantic (ETNA) using two surface tethered drifting sediment trap arrays with 7 trapping depths located between 100 and 600 m. Data on particulate matter fluxes were fitted to the normalized power function $F_z = F_{100} (z/100)^{-b}$, with F_{100} being the flux at a depth (z) of 100 m and b being the attenuation coefficient. Higher b-values suggest stronger flux attenuation and are influenced by factors such as faster degradation at higher temperatures. In this study, b-values of organic carbon fluxes varied between 0.74 and 0.80 and were in the intermediate range of previous reports, but lower than expected from seawater temperatures within the upper 500 m. During this study, highest b-values were determined for fluxes of particulate hydrolysable amino acids (PHAA), followed by particulate organic phosphorus (POP), nitrogen (PN), carbon (POC), chlorophyll *a,* and transparent exopolymer particles (TEP), pointing to a sequential degradation of organic matter components during sinking. Our study suggests that in addition to O_2 concentration, organic matter composition co-determines transfer efficiency through the mesopelagial. The magnitude of future carbon export fluxes may therefore also depend on how organic matter quality in the surface ocean changes under influence of warming, acidification, and enhanced stratification.

1. Introduction

The biological carbon pump, defined as the export of biologically fixed carbon dioxide (CO_2) from the surface to the deeper ocean mainly in the form of sinking particles (Volk and Hoffert, 1985), influences atmospheric CO_2 concentration and affects ecosystem structure and elemental distributions in the ocean. The total amount of carbon export as well as the efficiency of the biological carbon pump, *i.e.* the ratio between export and primary production, are highly dynamic (Buesseler and Boyd, 2009; Lam et al., 2011). Changes in the efficiency of the biological carbon pump may have been responsible for past atmospheric CO_2 variability between glacial-interglacial transition periods (Kohfeld and Ridgewell, 2009) and play a key role for future climate predictions (Heinze et al., 2015).

Most of the POM being exported below the surface mixed layer (<200m in general) is solubilized and remineralized within the mesopelagic layer, *i.e.* between depths of 200 and 1000 m (Bishop et al., 1978; Suess, 1980). The shallower the carbon remineralization depth, the more likely is CO_2 to exchange with the atmosphere, and hence drive a shorter carbon storage time in the ocean (Volk and Hoffert, 1985; Kwon et al., 2009). Factors driving export flux attenuation in the mesopelagic have therefore a large influence on CO_2 sequestration in the ocean. The vertical profile of sinking particulate organic carbon (POC) flux has often been described by a normalized power function: $F_z = F_{100}(z/100)^{-b}$, where F_z is the particle flux as a function of depth z, F_{100} is the flux at 100 m depth, and b is the flux attenuation coefficient (Martin et al., 1987; hereafter *M87*). The authors of the *M87* study derived an 'open ocean composite' for POC export fluxes from North Pacific data with a $F_{100} = 50.3$ mg m^{-2} d^{-1} and b = 0.86. However strong regional variations of both total export POC fluxes and b values are observed (Martin et al., 1987; Buesseler et al., 2007a; Torres Valdes et al., 2014; Marsay et al., 2015) with several factors proposed to control export flux attenuation. Increased attenuation, *i.e.* higher b-values, have been related to increased temperature (Marsay et al.,

6

217 2015), zooplankton feeding activity (Lampitt et al., 1990), coprophagy, coprorhexy, and

218 coprochaly (Belcher et al. 2016), microbial cycling (Giering et al., 2014) and lack of ballast

219 (LeMoigne et al., 2012). Decreased flux attenuation, *i.e.* lower *b*-values, and thus higher

220 transfer efficiencies (T_{eff}) have been associated to high particle sinking velocity depending on

221 plankton community composition, especially the presence of larger phytoplankton cells

222 (Buesseler, 1998; Buesseler and Boyd 2009), particle aggregates (Alldredge and Gotschalk,

223 1989), and fecal pellets (Cavan et al., 2015). Organic polymers, such as transparent

224 exopolymer particles (TEP) increase the rate of aggregate formation due to their high

225 stickiness (Alldredge et al., 1993; Engel, 2000; Passow, 2002; Chow et al., 2015) and

226 supposedly play an important role in particle export fluxes (Passow, 2002; Arrigo, 2007;

227 Chow et al., 2015). TEP are carbon-rich particles that form from dissolved polysaccharides

228 (Engel et al., 2004). When included in sinking POM inventories, TEP may increase carbon

229 relative to nitrogen export fluxes, a mechanism potentially counteracting rising CO_2

230 concentration in the atmosphere (Schneider et al., 2004; Arrigo, 2007; Engel et al., 2014).

231 However, TEP themselves are non-sinking due to a high water content and low density

232 (Azetzu-Scott and Passow, 2004), and little quantitative data are available on TEP export by

233 sinking particles so far (Passow et al., 2000; Martin et al., 2011; Ebersbach et al., 2014).

234 Thus, the role of TEP in carbon export is still unresolved.

235 Reduced POC flux attenuation has also been suggested for oxygen minimum zones (OMZs)

236 (Martin et al., 1987; Haake et al., 1992; Devol and Hartnett, 2001; Van Mooy et al., 2002;

237 Keil et al., 2015) as a consequence of reduced zooplankton feeding and microbial degradation

238 activities in suboxic (<5 μmol O_2 kg^{-1}) waters. So far, the vast majority of mesopelagic

239 downward POM flux measurements originate from well oxygenated waters (>100 μmol O_2

240 kg^{-1}). In the *M87* study, five sets of drifting sediment traps were deployed in the oxygenated

241 North Pacific and four sets were deployed in the Eastern Tropical North Pacific (ETNP)

242 OMZ. The flux attenuation coefficients (*b*) for the oxygenated North Pacific averaged 0.90 ±

Gelöscht: d

244 0.06, while lower *b* values averaging 0.66 ± 0.24 were measured in the ETNP OMZ. In

245 agreement, Devol and Hartnett (2001) and Van Mooy et al. (2002) observed low particle

246 attenuation in the OMZ of the ETNP off Mexico, yielding *b* coefficients of 0.36 and 0.40,

247 respectively. Keil et al. (2015) found *b* values of 0.59-0.63 in the suboxic Arabian Sea. These

248 studies thus indicate that a greater proportion of the sinking POM escapes degradation while

249 sinking through suboxic waters. However, influence of oxygen on organic matter degradation

250 may vary between individual components. For instance, degradation of hydrolysable amino

251 acid under suboxic conditions was found to continue with the same rate as compared to oxic

252 conditions (Van Mooy et al. 2002; Pantoja et al. 2004), suggesting that anaerobic and micro-

253 aerobic bacteria preferentially utilize nitrogen-rich components.

254

255 So far, little is known on sinking POM flux attenuation in hypoxic waters (<60 μmol O_2 kg^{-1}),

256 which are more widespread (~4% of ocean volume) compared to suboxic waters (< 0.05% of

257 ocean volume). Laboratory studies indicated that particle aggregates sinking through hypoxic

258 waters can become suboxic within their interior due to oxygen diffusion limitation and evolve

259 microbial degradation processes typical for suboxic waters (Alldredge and Cohen, 1987;

260 Ploug et al., 1997; Stief et al., 2016). For example, at an ambient O_2 concentration of 60 μmol

261 kg^{-1}, the O_2 uptake by a 2 mm (diameter) aggregate was diffusion-limited and a 0.5 mm wide

262 anoxic core occurred within its interior (Ploug and Bergkvist, 2015). Since OMZs are

263 expected to expand in the future as a consequence of global warming and altered circulation

264 patterns (Stramma et al., 2008), the role of oxygen in controlling the biological pump

265 efficiency needs to be better constrained for predicting ocean-climate feedbacks. In order to

266 assess what controls carbon flux attenuation and depth-related changes in sinking particle

267 composition in hypoxic waters, we determined downward POM fluxes in the ETNA off the

268 coast of Mauritania, which exhibits an extensive hypoxic OMZ between 300 and 500 m. We

269 used two parallel drifting, surface-tethered sediment trap devices with particle interceptor

Gelöscht: e

Gelöscht: drifting

8

272 traps (PITs) at 7-8 different depths between 60-600 m to estimate fluxes to and within the

273 OMZ.

274

275

276 **2. Methods**

277 2.1. The Study area

278 The study was conducted from March 17th to April 16th 2014 during a cruise of the RV

279 METEOR to the ETNA region off the coast of Mauritania (Fig. 1a). The study area included

280 hypoxic waters with minimum values of oxygen concentration of 40 μmol kg^{-1} as determined

281 by CTD (Seabird) casts with two calibrated oxygen sensors at midwater depths of 350-500 m

282 (Fig. 1b) (Visbeck, 2014).

283

284 2.2. Sediment trap operation and sample analysis

285 Free-drifting surface-tethered sediment trap devices were deployed for 196 h during the first

286 deployment and 281h during the second deployment (Fig. 1c). The first trap device was

287 deployed on the 24th of March 2014 (11:00 UTC) at 10.00°N 21.00°W with 12 Particle-

288 Interceptor-Traps (PITs) at each of 8 depths: 60, 100, 150, 200, 300, 400, 500, and 600 m.

289 The device was recovered on the 1st of April 2014 (14:30 UTC) at 10.46°N 21.39°W. The

290 second device was deployed on the 27th of March 2014 (16:00 UTC) at 10.25°N 21°W with

291 12 PITs at each of 7 depths: 100, 150, 200, 300, 400, 500, and 600 m. The second trap device

292 was recovered on the 8th of April 2014 (09:00 UTC) at 10.63°N 21.50°W. Both devices

293 slowly drifted northwest and were recovered approximately 37 nm away from their

294 deployment location (Fig. 1c). Within the drifting area oxygen concentration in the OMZ

295 resembled the overall pattern of the Mauritanian upwelling with fully hypoxic conditions

296 between 300 and 500 m (Fig. 1d).

Gelöscht: e

Gelöscht:

Gelöscht: e

9

300   The design of the trap devices and the drifting array basically follows Knauer et al. (1979),

301   with 12 PITs mounted on a polyvinylchloride (PVC) cross frame. The PITs were acrylic tubes

302   with an inside diameter of 7 cm, an outside diameter of 7.6 cm and a height of 53 cm, leading

303   to an aspect ratio of 7.5. The aspect ratio and a baffle system consisting of smaller acrylic

304   tubes attached to the top end of each PIT help to reduce drag-induced movement within the

305   trap (Soutar et al., 1977). PVC crosses with PITs were attached to a free-floating line, which

306   was buoyed at the surface and weighed at the bottom. The surface buoys of the arrays carried

307   GPS/Iridium devices and flashlights.

308   Prior to each deployment, each PIT was filled with 1.5 L filtered surface seawater (0.2 μm

309   pore size cartridge) collected from the ship's underway seawater system, up to 3/4 of the

310   PITs' height. A brine solution was prepared by dissolving 50 g L^{-1} sodium chloride with

311   filtered surface seawater and subsequently filtered through a 0.2 μm cartridge to remove

312   excess particulates. 20 ml of formalin was then added per L of the solution to achieve a brine

313   solution with 2% formalin. The preservative solution was then slowly transferred into each

314   PIT beneath the 1.5 L of filtered seawater using a peristaltic pump. PITs were covered with

315   lids immediately, to minimize contamination before deployment.

316   Sample treatment after trap recovery followed recommendations given by Buesseler et al.

317   (2007b). After recovery, all PITs were capped to minimize contamination. The density

318   gradient was visually inspected and found intact at the position of prior to deployment or at a

319   maximum 2 cm above. Then, seawater was pumped out of each PIT using a peristaltic pump

320   down to 2-3 cm above the density gradient. The remaining ~0.6 L were subsequently

321   transferred to canisters, pooled from 11 tubes per depth. 40 ml formalin were added to each

322   canister. Samples from each depth were passed through a 500 μm nylon mesh. Swimmers

323   were removed from the mesh with forceps under a binocular microscope and the remaining

324   particles, which stuck to the mesh, were transferred back to the sample. Samples were

325   subsequently split into aliquots of the total sample. Therefore, the pooled sample was

326   transferred into a round 10 L canister and stirred at medium velocity with a magnetic bar.

327   Aliquots were transferred into 0.5 L Nalgene bottles with a flexible tube using a peristaltic

328   pump. Aliquots of samples were filtered under low pressure (<200 mbar) onto different filter

329   types (combusted GF/F 0.7 μm, polycarbonate 0.4 μm, or cellulose acetate 0.8 μm; see below)

330   for different analyses and stored frozen (-20 °C) until analyses.

331

332   2.2.1. Biogeochemical Analyses

333   The following parameters were determined: Total particulate mass (TPM), particulate organic

334   carbon (POC), particulate nitrogen (PN), particulate organic phosphorus (POP), biogenic

335   silica (BSi), chlorophyll *a* (Chl *a*), particulate hydrolysable amino acids (PHAA) and

336   transparent exopolymer particles (TEP).

337

338   TPM was analyzed in triplicate. The following aliquots were filtered in triplicate onto pre-

339   weighed 0.4 μm polycarbonate filters: 800 ml (2 x 400 ml; 8 % of total sample) for the depths

340   of 600 m to 300 m of deployment #1, 400 ml (4 % of total sample) for the depths of 200 m

341   and 150 m of deployment #1 and for all depths of deployment #2, 420 ml (4 % of total

342   sample) for the depth of 100 m and 60 m of deployment #1. Filters were rinsed two times

343   with Milli-Q water, dried at $60^{°}$C for 4 h and stored until weight measurement on a Mettler

344   Toledo XP2U microbalance.

345

346   POC and PN aliquots were filtered in triplicate onto combusted (8h at 500°C) GF/F filters

347   (Whatmann, 25 mm): 400 ml (4 % of total sample) for the depths of 600 m to 150 m of

348   deployment #1, 420 ml (4 % of total sample) for the depths of 100 m and 60 m of deployment

349   #1, 100 ml (1 % of total sample) for all depths of deployment #2. For the depths of 150 m,

350   100 m and 60 m of deployment #1, 400 - 420 ml (4 % of total sample) was filtered onto two

351   filters, due to the high particle load at these depths. Filters were exposed to fuming

352 hydrochloric acid in a fuming box over night to remove carbonate and subsequently dried

353 (60°C, 12 h). For analysis, the filters were enclosed in tin cups and analysed using an Euro

354 EA elemental analyzer calibrated with an acetanilide standard. For the depths of 150, 100 and

355 60 m of deployment #1 the sum of both filters was taken.

356

357 POP was determined in triplicate, except for 60 m depth of deployment #1, which was only

358 determined in duplicate. The following aliquots were filtered onto combusted GF/F filters

359 (Whatmann, 25 mm): 400 ml (4 % of total sample) for the depths of 600 m to 150 m of

360 deployment #1, 420 ml (4 % of total sample) for the depths of 100 m and 60 m of deployment

361 #1, 100 ml (1 % of total sample) for all depths of deployment #2. For the depths of 200 m to

362 60 m of deployment #1, the volume of 400 ml/ 420 ml (4 % of total sample) was filtered onto

363 two filters, due to the high particle load at these shallower depths. Organic phosphorus

364 collected on the filters was digested in the potassium peroxydisulphate-containing substance

365 Oxisolv (Merck) for 30 min in a pressure cooker and measured colorimetrically as ortho-

366 phosphate following the method of Hansen and Koroleff (1999).

367

368 PHAA were determined in duplicate. The following aliquots were filtered onto combusted

369 GF/F filters (25 mm): 400 ml (4 % of total sample) for the depths of 600 m to 150 m of

370 deployment #1, 420 ml (4 % of total sample) for the depths of 100 m and 60 m of deployment

371 #1, 100 ml (1 % of total sample) for all depths of deployment #2. For the depths of 150 m,

372 100 m and 60 m of deployment #1, the volume of 400 ml / 420 ml (4 % of total sample) was

373 filtered onto two filters, due to the high particle load at these shallower depths. PHAA

374 analysis was performed according to Lindroth & Mopper (1979) and Dittmar et al. (2009)

375 with some modifications. Duplicate samples were hydrolyzed for 20 h at 100°C with

376 hydrochloric acid (30%, Suprapur, Merck) and neutralized by acid evaporation under vacuum

377 in a microwave at 60°C. Samples were washed with water to remove remaining acid.

Gelöscht: wrapped

Gelöscht: foil

Gelöscht: in

Gelöscht:

382 Analysis was performed on a 1260 HPLC system (Agilent). Thirteen different amino acids

383 were separated with a C18 column (Phenomenex Kinetex, 2.6 μm, 150 x 4.6 mm) after in-line

384 derivatization with o-phtaldialdehyde and mercaptoethanol. The following standard amino

385 acids were used: aspartic acid (AsX), glutamic acid (GlX), histidine (His), serine (Ser),

386 arginine (Arg), glycine (Gly), threonine (Thr), alanine (Ala), tyrosine (Tyr), valine (Val),

387 phenylalanine (Phe), isoleucine (Ileu), leucine (Leu), γ- amino butyric acid (GABA). α-

388 amino butyric acid was used as an internal standard to account for losses during handling.

389 Solvent A was 5% acetonitrile (LiChrosolv, Merck, HPLC gradient grade) in

390 sodiumdihydrogenphospate (Merck, suprapur) buffer (pH 7.0), Solvent B was acetonitrile. A

391 gradient was run from 100% solvent A to 78% solvent A in 50 minutes. The detection limit

392 for individual amino acids was 2 nmol monomer L^{-1}. The precision was <5%, estimated as the

393 standard deviation of replicate measurements divided by the mean. The degradation index

394 (DI) was calculated from the amino acid composition following Dauwe et al. (1999).

395

396 BSi was determined in triplicate. The following aliquots were filtered onto cellulose acetate

397 filters (0.8 μm): 400 ml (4 % of total sample) for the depths of 600 m to 150 m of deployment

398 #1, 420 ml (4 % of total sample) for the depths of 100 m and 60 m of deployment #1, 200 ml

399 (2 x 100 ml; 2 % of total sample) for all depths of deployment #2. Filters were incubated with

400 25 ml NaOH (0.1 M) at 85°C for 2h 15min in a shaking water bath. After cooling of the

401 samples, analysis was conducted according to the method for determination of $Si(OH)_4$ by

402 Hansen and Koroleff (1999). Fluxes of biogenic opal were calculated assuming a water

403 content of ~10% and therefore the chemical formula SiO_2 x $0.4H_2O$ with a density of ~2.1 g

404 cm^{-3} (Mortlock and Fröhlich 1989).

405

406 Chl *a* was determined in duplicate. The following aliquots were filtered onto GF/F filters (25

407 mm): 400 ml (4 % of total sample) for the depths of 600 m to 150 m of deployment #1, 420

409   ml (4 % of total sample) for the depths of 100 m and 60 m of deployment #1, 100 ml (1 % of

410   total sample) for all depths of deployment #2. For the depths of 200 m to 60 m of deployment

411   #1, the volume of 400 ml / 420 ml (4 % of total sample) was filtered onto two filters, due to

412   the high particle load at these shallower depths. Samples were analyzed after extraction with

413   10ml of acetone (90%) on a Turner fluorimeter after Welschmeyer (1994). Calibration of the

414   instrument was conducted with spinach extract standard (Sigma Aldrich).

415

416   TEP were determined in quadruplet by microscopy after Engel (2009). Between 3.5 and 10 ml

417   (0.03-0.1% of total sample) for the depths of deployment #1 and #2 were filtered onto 0.4 μm

418   Nuclepore membrane filters (Whatmann) and stained with 1 mL Alcian Blue solution. Filters

419   were mounted onto Cytoclear© slides and stored at -20 °C until microscopy analysis using a

420   light microscope (Zeiss Axio Scope A.1) connected to a camera (AxioCAM Mrc). Filters

421   were screened at 200x magnification. 30 pictures were taken randomly from each filter in two

422   perpendicular cross sections (15 pictures each; resolution 1040 x 1040 pixel, 8-bit color

423   depth). Image analysis software WCIF ImageJ (Version 1.44, Public Domain, developed at

424   the US National Institutes of Health, courtesy of Wayne Rasband, National Institute of Mental

425   Health, Bethesda, Maryland) was used to semi-automatically analyse particle numbers and

426   area.

427

428   The carbon content of TEP (TEP-C) was estimated after Mari (1999) using the size dependent

429   relationship:

430

431   TEP-C = a Σ_i (n_i r_i^D),   (1)

432

433   with n_i being the number of TEP in the size class i and r_i the mean equivalent spherical radius

434   of the size class. The constant a = 0.25 * 10^{-6} (μg C) and the fractal dimension of aggregates

435 D= 2.55 were proposed by Mari (1999). TEP-C was only calculated for the size fraction <5

436 µm including mainly free TEP, because larger TEP included TEP covered aggregates with

437 solid particles. Estimating carbon content of these larger particles would overestimate TEP-C

438 as the volume of the other particles would be included.

439

440 2.3. Calculations and statistics

441 Fluxes of $CaCO_3$ and lithogenic matter (lith) were calculated as:

442

443 $[CaCO_3+ lith] = [TPM]-[POM]-[Opal],$ (2)

444

445 Total mineral ballast ($ballast_{total}$) was calculated as:

446

447 $[ballast_{total}]= [TPM]-[POM],$ (3)

448

449 and the percentage of $ballast_{total}$ ($\%ballast_{total}$) was calculated as:

450

451 $[\%ballast_{total}] =([TPM] - [POM])/[TPM]*100,$ (4)

452

453 The transfer efficiency (T_{eff}) of particulate components was calculated as the ratio of fluxes at

454 600 m to those at 100 m.

455

456 Calculated mean values include replicate measurements of both deployments. Data fits and

457 statistical tests were performed with the software packages Microsoft Office Excel 2010,

458 Sigma Plot 12.0 (Systat) and Ocean Data View (ODV) (Schlitzer, 2013). Weighted-average

459 gridding was used in ODV to display data according to data coverage with automatic scale

460 lengths. The overall significance level was $p < 0.05$.

15

461

462

3. Results and Discussion

464

3.1. Fluxes of different compounds

Export fluxes of TPM and particulate organic elements determined during both trap
deployments showed good overall agreement and a decrease with depth, fitting well to the
power law function of *M87* (Fig. 2a-d, Fig.3a-d and Table 1). Averaging fluxes from both
deployments yielded a total mass flux of 240 $\pm$ 34 mg m^{-2} d^{-1} at 100 m decreasing to 141 $\pm$
8.8 mg m^{-2} d^{-1} in the core of the OMZ (400 m) (Fig. 2a). Fluxes of POC, PN and POP at 100
m depth were 73 $\pm$ 8.8, 13$\pm$ 1.4 and 0.67 $\pm$ 0.06 mg m^{-2} d^{-1}, respectively, and decreased to 26
$\pm$ 4.5, 3.0 $\pm$ 0.41 and 0.19 $\pm$ 0.04 mg m^{-2} d^{-1} at 400 m depth (Fig. 2b-d). The contribution of
POC flux to total mass flux (% OC) decreased from about 30% at 60-150 m depth to 17-20%
at 400 m depth and showed only a minor decrease below 400 m, to 14-16% at 600 m depth.
Similarly, the percentage of PN flux to total mass flux (% N) showed the largest decrease
between 60 and 400 m, i.e. from 6.6% to 2.0-2.3%, and less decline below, reaching 1.7-1.8%
at 600 m. The percentage of POP flux to total mass flux (% P) decreased from 0.37% at 60 m
depth to 0.11-0.16% at 400 m depth, and remained constant below 400 m depth. No previous
data are available for POM export fluxes at our study site for direct comparison. However,
our trap data compare well to carbon export fluxes estimated from particle size data (i.e. 10-
300 mg C m^{-2} d^{-1}) reported for 100 m depth in the area off Cape Blanc (Mauritania) by
Iversen et al. (2010).

483

Fluxes of phytoplankton biomass, as indicated from Chl *a*, were similar at 100 m during both
deployments, with 104 $\pm$ 1.5 μg Chl *a* m^{-2} d^{-1} during the first and 116 $\pm$ 6.2 μg m^{-2} d^{-1} during
the second deployment, but behaved differently below, with a stronger flux attenuation above

487 the OMZ during the first compared to the second deployment (Fig. 3a). Fluxes within the

488 OMZ core were 35 ± 0.1 µg m^{-2} d^{-1} (#1) and 53 ± 0.5 µg m^{-2} d^{-1} (#2) respectively.

489

490 Opal fluxes were also similar during both deployments, yielding an average of 47 ± 3.6 mg m^{-2}

491 d^{-1} at 100 m, steadily decreasing to 32 ± 2.4 mg m^{-2} d^{-1} at 400 m depth (Fig. 3b). Similar to

492 Chl *a*, opal fluxes were slightly higher above the OMZ during the second compared to the

493 first deployment, but quite similar or even lower below the OMZ. This may indicate that the

494 second trap device, which drifted more northerly (Fig. 1c), exploited waters of a more recent

495 diatom bloom compared to the first deployment.

496 Fluxes of [CaCO$_3$ + lith] were similar to opal fluxes during the first deployment (F$_{100}$=52 mg

497 m^{-2} d^{-1}) but considerably lower during the second (F$_{100}$=14.8 mg m^{-2} d^{-1}) (data not shown).

498

499 During this study, export fluxes of TEP were estimated from decrease over depth of total

500 particle area and showed the strongest depth attenuation between 60 and 100 m during the

501 first deployment (Fig. 3c). Like Chl *a* fluxes, TEP export fluxes were slightly higher during

502 the second compared to the first deployment. At 100 m depth, average TEP flux was $1860 \pm$

503 46 cm^2 m^{-2} d^{-1} and decreased to 1190 ± 52 cm^2 m^{-2} d^{-1} at 400 m. Using a TEP size to carbon

504 conversion according to Mari (1999) yielded to an average TEP-C (<5 µm) flux of $1.73 \pm$

505 0.35 mg C m^{-2} d^{-1} at 100m depth, slightly decreasing to 1.64 ± 0.28 mg m^{-2} d^{-1} at 400 m and

506 further to 0.90 ± 0.32 mg m^{-2} d^{-1} at 600 m. Although TEP supposedly play an important role

507 in particle export fluxes (Passow, 2002; Arrigo, 2007; Chow et al., 2015), only a few previous

508 estimates for TEP export fluxes based on sediment traps have been given so far to which we

509 can compare our data. Martin et al. (2011) measured TEP export fluxes during a spring

510 bloom in the Iceland Basin (Northeast Atlantic Ocean) using the PELAGRA neutrally

511 buoyant sediment traps and determined values in the range of 30-120 mg Gum Xanthan

512 Equivalent m^{-2} d^{-1}. Ebersbach et al. (2014) obtained lower values of 0.03-5.14 mg Gum

515 Xanthan Equivalent m^{-2} d^{-1} during the LOHAFEX iron fertilization experiment in the

516 Southern Ocean. Assuming a conversion factor of 0.63 µg C µg^{-1} Gum Xanthan after Engel

517 (2004), these previous estimates suggest TEP-C export fluxes ranging from 0.02 to 3 mg m^{-2}

518 d^{-1} for the Southern Ocean and from 19 to 75 mg m^{-2} d^{-1} for the North Atlantic spring bloom.

519 Our data on TEP export fluxes for ETNA region are within the range of these previous

520 studies, but closer to the lower estimates for the Southern Ocean. It has to be emphasized,

521 though, that our calculated TEP-C fluxes are likely underestimates, since only suspended, i.e.

522 'free' TEP < 5 µm were taken into account. TEP-C associated to aggregates cannot be

523 determined with the applied microscopic technique. Overall, TEP-C export fluxes in the

524 ETNA were significantly related to Chl *a* fluxes, yielding [TEP-C, mg m^{-2} d^{-1}] = 11.9 [Chl *a*;

525 mg m^{-2} d^{-1}] + 0.74 (r²=0.59, n= 15, p<0.01).

526

527 A strong decrease at shallow depth (60–100 m) was also observed for PHAA fluxes during

528 the first deployment (Fig. 3d). Average PHAA fluxes were 330 ± 51 µmol m^{-2} d^{-1} at 100 m,

529 and 90 ± 20 µmol m^{-2} d^{-1} in the OMZ core at 400 m. These fluxes are equivalent to amino

530 acid related fluxes of 16.8 ± 2.6 mg C m^{-2} d^{-1} (100 m) and 4.48± 1.0 mg C m^{-2} d^{-1} (400 m),

531 respectively, which are typical values for PHAA-C fluxes in the ocean (Lee and Cronin,

532 1984). PHAA fluxes decreased slightly within the OMZ, i.e. from 300 to 500 m.

533

534

535 3.2. Flux attenuation in the ETNA OMZ

536 Fluxes from both deployments were fitted to the exponential decrease model (Martin et al.,

537 1987) and attenuation coefficients (*b*-values) were estimated for all components (table 1).

538 Higher *b*-values suggest stronger attenuation and may hint to either reduced sinking velocities

539 of particles or to faster degradation of more labile components. During this study, PHAA

540 were the most rapidly attenuated components of sinking particles, followed by POP, PN,

557 POC, Chl *a,* and TEP (table 1). Attenuation of mineral fluxes was less pronounced than for

558 TPM.

559 Attenuation coefficient of POC export fluxes was 0.80 during the first and 0.74 during the

560 second deployment. These values are in the intermediate range of previously determined *b-*

561 values for POC attenuation in the mesopelagic, shown to vary between 0.51 as determined in

562 the North Pacific (K2) and 1.59 as determined for the NASG (Buesseler et al., 2007a; Marsay

563 et al., 2015). Based on trap data from fully oxygenated water columns, Marsay et al. (2015)

564 recently suggested a linear relationship between POC flux attenuation and median water

565 temperature within the upper 500m of the water column according to: $b=0.062T+0.303$.

566 Applying this relationship to our study area, with temperature decreasing from 26°C at the

567 surface to 9°C at 500 m and a median temperature value of 12.01°C, would give a *b*-value of

568 1.05. This estimated *b*-value is higher than the values observed in this study (0.74 - 0.80) and

569 suggests that oxygen deficiency may reduce attenuation of POC fluxes in the ETNA resulting

570 in higher T_{eff} of organic matter though the OMZ's compared to well oxygenated waters.

571

572 Differences in flux attenuation coefficients translate into different T_{eff} for individual

573 components, with PHAA being the least and TEP being the most efficiently exported organic

574 component (table 1). In particular, values of T_{eff} for TEP and therewith for TEP-C were about

575 three times higher than for PHAA-C and even clearly higher than for bulk POC, suggesting a

576 preferential export of carbon included in TEP below 100 m. However, a steep decrease of

577 TEP flux was observed between 60 m and 100 m during the first deployment. TEP are

578 produced by a variety of organisms, i.e. different phytoplankton and bacterial species and

579 cannot be considered as of homogenous composition. Several mechanisms may therefore be

580 responsible for a change in TEP transfer efficiency with depth: 1) change of TEP

581 degradability with depth, 2) differences in TEP composition over depth related to association

582 with particles of different settling speed, 3) new production of TEP, abiotically or by bacteria,

583 during solubilization and degradation of sinking particles, 4) capture of suspended TEP by

584 sinking aggregates, or 5) reduced degradation rate of TEP at lower oxygen. In support of the

585 latter hypothesis, an attenuation of TEP fluxes within the OMZ (300-500 m) was not

586 detectable, but rather occurred again below the OMZ.

587

588 3.3. Changes in POM composition during export

589 POM, assumed to be $2.2 \times$ [POC] following Klaas and Archer (2002) made the greatest

590 contribution to TPM flux at 60 m, but decreased below. Conversely, [%ballast$_{total}$] increased

591 with depth, namely from 30% w/w at 60 m to 68% w/w at 600 m.

592 Biogenic opal (density: 2.1 g cm^{-3}) in the ocean is produced mainly by diatoms and

593 radiolarians. During this study, opal made a rather constant contribution to TPM fluxes with

594 20-25% weight below 100 m. Hence, the observed increase in the [%ballast$_{total}$] with depth

595 was due to an increasing contribution of $CaCO_3$ and lithogenic material. [$CaCO_3$+ lith] to

596 TPM increased from 10-15% above 150 m to 45% at 600 m. As a consequence, the ballast

597 ratio, defined as [Opal]:[$CaCO_3$+lith] changed from a dominance of opal above the OMZ to a

598 dominance [$CaCO_3$+lith] within and below the OMZ (Figure 4). Slight differences were

599 observed between the two deployments. Contribution of opal and of [$CaCO_3$+lith] to TPM at

600 100m was almost equal during the first deployment with a share of 18% and 22%,

601 respectively. During the second deployment the contribution of opal to TPM at 100 m was

602 21% but only 6% for [$CaCO_3$+lith]. Thus, the higher contribution of opal to TPM fluxes

603 together with higher Chl *a* fluxes indicated that diatomaceous material had a higher share of

604 particles sinking out of the euphotic zone down to the OMZ core during the second compared

605 to the first deployment.

606

607 Molar [POC]:[PN] ratios were close to the Redfield ratio at depths shallower than 100 m,

608 increased to a ratio of 10 at 400 m depth and remained constant between 400 and 600 m

Gelöscht: O

20

610 depth (Fig. 5a). [PN]:[POP] ratios were much above Redfield, with values varying between

611 30 and 45 throughout the water column (Fig. 5b). Also [POC]:[POP] ratios were much higher

612 than Redfield ratios, and showed an increasing trend down to 300-400 m depth, while

613 decreasing below (Fig. 5c). These changes in elemental ratios suggested a preferential

614 remineralization of POP in the upper 300 m, followed by PN and POC deeper down.

615 The percentage of total organic matter in TPM fluxes decreased from 67% at 100m to 32% at

616 600m (Fig. 6d). As a consequence of higher T_{eff} of TEP relative to bulk POC, contribution of

617 TEP-C to POC increased significantly with depth during both deployments (p<0.01; r²=0.59,

618 n=15) and was 2% at 100 m, and 6% within and 5% below the OMZ (Fig. 5e). Because TEP

619 do not sink by themselves their export to depth depends on their incorporation into settling

620 aggregates. In a laboratory study, Engel et al. (2009) observed that decomposition of TEP was

621 faster relative to bulk POC for aggregates formed from calcifying and non-calcifying

622 *Emiliania huxleyi* cultures. In that experiment, aggregate decomposition was investigated

623 under oxic conditions. Other studies also showed fast microbial degradation of TEP under

624 oxic conditions (Bar-Zeev and Rahav, 2015). One possible explanation for increasing [TEP-

625 C]:[POC] in the hypoxic OMZ of the ETNA region could be that TEP are mostly included in

626 sinking aggregates, whereas POC could be included in various particle types, such as large

627 cells, detritus or fecal pellets. Ploug et al. (1997) estimated that carbon turn-over time inside

628 anoxic aggregates can be strongly reduced. Due to high microbial activity and reduced water

629 exchange aggregates sinking into hypoxic waters are more likely to experience anoxic

630 conditions than individual particles (Ploug and Bergkvist, 2015). Thus, TEP settling into

631 hypoxic waters by aggregates may be exposed to anoxia, and therewith to reduced microbial

632 degradation, in consequence leading to a preferential TEP transfer through the OMZ. This

633 may also explain the decrease of [TEP-C]:[POC] ratios below the OMZ at 600 m water depth,

634 which was, however, only observed during the second deployment. Since PN was more

Gelöscht: observed

636   rapidly degraded than POC this also implied that the ratio of [PN]:[TEP-C] became lower

637   with depth.

638

639   In contrast to [TEP-C]:[POC], values of [PHAA-C]:[POC] in POM fluxes declined during

640   both deployments above the OMZ. However, in the core of the OMZ, at 400 m, [PHAA-

641   C]:[POC] was higher than at 300 and 500 m (Fig. 5f); the same pattern was also observed

642   for [PHAA-N]:[PN] (data not shown). A faster decline in PHAA in sinking particles mainly

643   above but not within the OMZ is different to observations gained for more extensively

644   oxygen-deficient to full anoxic waters of the Eastern Tropical south Pacific (ETSP), which

645   suggested that PHAA are preferentially degraded under low oxygen conditions (Van Mooy et

646   al., 2002). In those studies, total hydrolysable amino acid (THAA) degradation under anoxic

647   conditions was found to continue with the same rate compared to oxic conditions, while

648   degradation of non-amino acid compounds was found to slow down (Pantoja et al., 2004; Van

649   Mooy et al., 2002). A preferential degradation of nitrogen-rich compounds over POC suggests

650   that microbes degrading organic matter under strongly oxygen deficient conditions via

651   denitrification preferentially utilize nitrogen-rich amino acids (Van Mooy et al., 2002). Our

652   data on PHAA do not suggest preferential amino acid loss due to components of sinking POM

653   degradation in the ETNA OMZ. This is in accordance with the absence of microbial N-loss

654   processes/ absence of denitrifying bacteria in ETNA oxygen deficient waters (Löscher et al.,

655   2016). Instead, a slight increase of [PHAA-C]:[POC] in the OMZ may point to higher protein

656   production by bacterial growth as previously observed for mesopelagic waters (Lee and

657   Cronin, 1982, 1984) and may be related to increased growth efficiency of bacteria

658   experiencing low oxygen condition as suggested by Keil et al. (2016).

659

660   Among all amino acids determined, GlX, Gly, Gaba and Leu showed the most pronounced

661   variations with depth (Fig. 6a-d, table 2). Whereas GlX and Leu showed a decrease with

662 depth (Fig. 6a, c), Gly continuously increased. It has been shown that Gly is enriched in the

663 silica-protein complex of diatom frustules (Hecky et al., 1973). Preservation of frustules

664 relative to POM may therefore explain the relative increase of Gly with depth in sinking

665 particles. GlX has been used as a biomarker (Abramson et al., 2010), since GlX was shown to

666 be enriched in calcerous plankton (Weiner and Erez, 1984). During this study %Mol of GlX

667 was higher during the first deployment, which is in accordance with the observed higher

668 contribution of [$CaCO_3$+lith] to TPM flux. Gaba has been used as an indicator for bacterial

669 decomposition activity (Lee and Cronin, 1982; Dauwe and Middelburg, 1998; Engel et al.,

670 2009). During this study %Mol Gaba behaved differently during the first compared to the

671 second deployment with similar values within the OMZ, a pattern also observed for opal

672 fluxes (Fig. 3b). Moreover, %Mol of Gaba showed a local peak at 300 m, i.e. within the

673 upper oxycline, and may point to high bacterial activity at this depth. Leu is an essential

674 amino acids and readily taken up by heterotrophic microorganisms. Little change in %Leu in

675 the OMZ core (Fig. 3d) compared to above (<300 m) indicated reduced microbial reworking

676 of organic matter under hypoxic conditions. Another indication of microbial reworking of

677 organic matter can be derived from the Degradation index (DI) (Dauwe et al., 1999). During

678 this study, the DI decreased with increasing depth, but with differences between the

679 deployments (Fig. 7). During #2, DI was slightly higher above the OMZ indicating fresher

680 material. During #1 DI did not decrease within the OMZ, but it continued to decrease from

681 300 m to 500 m depth during deployment #2. Together with observations on Chl *a* and opal

682 fluxes, as well as changes in ballast ratio, data on DI suggest that the particles of more

683 diatomaceous origin likely continued to decompose under hypoxic conditions.

684

685

686 **4. Conclusions**

687 Despite an improvement in understanding principle processes and drivers of particle export

688 processes over the past decades, spatial and temporal variability of export fluxes in the ocean

689 are still difficult to predict. This is partly due to the lack of observations in different regions

690 of the mesopelagic realm. Our study is the first to describe fluxes of POM in the hypoxic

691 mesopelagic waters of the ETNA. Our data suggest a higher transfer efficiency than expected

692 from seawater temperature solely, suggesting reduced degradation of organic matter by

693 heterotrophic communities at low oxygen concentration (<60 µmol O_2 kg^{-1}). The biological

694 carbon pump in high productivity regimes associated to OMZs, i.e. Eastern Boundary

695 Upwelling Systems such as the ETNA region off Mauritania, may therewith be more efficient

Gelöscht: e

696 than in fully oxygenated waters of comparable temperature. In contrast to suboxic systems ($<$

697 5 µmol O_2 kg^{-1}) a relatively higher loss of amino acids from POM fluxes was not evident for

698 the hypoxic water-column, suggesting microbial N-loss processes were comparatively minor

699 within particles. This, however, requires further investigation since no corresponding rate

700 measurements of denitrification or anammox were conducted during this study. Organic

701 matter composition seems to have a large impact on transfer efficiencies as carbon fluxes

702 associated to amino acids were much more attenuated over depth than carbon fluxes

703 associated to polysaccharide-rich TEP. If these findings are transferable to other oceanic

704 regions, changes in surface ocean organic matter composition in response to climate change

705 may also impact the carbon remineralization depth and therewith may have a feed-back

706 potential to atmospheric CO_2 concentration that yet has to be assessed.

707

708 **5. Competing interest**

709 The authors declare that they have no conflict of interest.

710

711 **6. Acknowledgements**

24

724 **References**

725

726 Abramson, L., Lee, C., Liu, Z.F., Wakeham, S.G., and Szlosek, J.: Exchange between

727 suspended and sinking particles in the northwest Mediterranean as inferred from the organic

728 composition of in situ pump and sediment trap samples. Limnol. Oceanogr., 55, 2, 725-739,

729 doi: 10.4319/lo.2009.55.2.0725, 2010.

730

731 Alldredge, A. L. and Cohen, Y.: Can microscale chemical patches persist in the sea?

732 Microelectrode study of marine snow, fecal pellets. Science, 235, 4789, 689-91, 1987.

733

734 Alldredge, A. L., and Gotschalk, C. C.: Direct observation of the mass flocculation of diatom

735 blooms: characteristics, settling velocities and formation of diatom aggregates. Deep-Sea

736 Research, 36, 159–171, 1989.

737

738 Alldredge, A. L., U. Passow, and Logan, B. E.: The abundance and significance of a class of

739 large, transparent organic particles in the ocean. Deep-Sea Res. 40, 1131–1140, 1993.

740

741 Arrigo, K. R.: Carbon cycle - Marine manipulations. NATURE, 450, 7169, 491-492, 2007.

742

743 Azetsu-Scott, K., and Passow, U.: Ascending marine particles: Significance of transparent

744 exopolymer particles (TEP) in the upper ocean. Limnol. Oceanogr. 49, 3, 741-748, 2004.

745

746 Bar-Zeev, E., and Rahav, E.: Microbial metabolism of transparent exopolymer particles

747 during the summer months along a eutrophic estuary system. Frontiers in Microbiol. 6, 403,

748 doi: 10.3389/fmicb.2015.00403, 2015.

749

750

751 Belcher, A., Iversen, M., Manno, C., Henson, S. A., Tarling, G. A., and Sanders, R.: The role

752 of particle associated microbes in remineralization of fecal pellets in the upper mesopelagic of

753 the Scotia Sea, Antarctica. Limnol. Oceanogr. 61, 3, 1049-1064, doi: 10.1002/lno.10269 ,

754 2016

755

756 Bishop, J. K. B., Ketten, D. K., and Edmon, J. M.: The chemistry, biology and vertical flux of

757 particulate organic matter from the upper 400 m of the Cape Basin in the southeast Atlantic

758 Ocean. Deep-Sea Res. 25, 1121-1161, 1978.

759

760 Buesseler, K. O.: The decoupling of production and particulate export in the surface ocean.

761 Global Biogeochem. Cycles 12:297-310, 1998.

762

763 Buesseler, K.O., C.H. Lamborg, P.W. Boyd, P.J. Lam, T.W. Trull, R.R. Bidigare, J.K.B.

764 Bishop, K.L. Casciotti, F. Dehairs, M. Elskens, M. Honda, D.M. Karl, D.A. Siegel, M.W.

765 Silver, D.K. Steinberg, J. Valdes, B. Van Mooy, and Wilson S.: Revisiting carbon flux

766 through the ocean's twilight zone. Science, 316, 567–570, 2007a

767

768 Buesseler, K.O., Antia, A., Chen, M., Fowler, S. W., Gardner, W.D., Gustafsson, O., Harada,

769 K., Michaels, A.F., van der Loeff, M. R., Sarin, M., Steinberg, D. K. and Trull, T.: An

770 assessment of the use of sediment traps for estimating upper ocean particle fluxes. Journal of

771 Marine Research, 65, 345-416, 2007b.

772

773 Buesseler, K.O., and Boyd P.W.: Shedding light on processes that control particle export and

774 flux attenuation in the twilight zone. Limnol. Oceanogr., 54, 4, 1210–1232, 2009

775

Gelöscht: ,

777 Cavan, E.L., Le Moigne, F. A. C., Poulton, A. J., Tarling, G. A., Ward, P., Daniels, C. J.,

778 Fragoso, G. M., and Sanders, R. J. : Attenuation of particulate organic carbon flux in the

779 Scotia Sea, Southern Ocean, is controlled by zooplankton fecal pellets. Geophys. Res. Lett.,

780 42, 3, 821-830, doi: 10.1002/2014GL062744, 2015

781

782 Chow, J. S., Lee, C. and Engel, A.: The influence of extracellular polysaccharides, growth

783 rate, and free coccoliths on the coagulation efficiency of *Emiliania huxleyi*. Mar. Chem., 175,

784 2015.

785

786 Dauwe, B., and Middelburg, J.J.: Amino acids and hexosamines as indicators of organic

787 matter degradation state in North Sea sediments. Limnol. Oceanogr. 43, 782-798, 1998.

788

789 Dauwe, B., Middelburg, J. J., Herman, P. M. J., and Heip, C. H. R.: Linking diagenetic

790 alteration of amino acids and bulk organic matter reactivity. Limnol. Oceanogr. 44, 1809–

791 1814, 1999.

792

793 Devol, A.H. and Hartnett, H. E.: Role of the oxygen minimum zone in transfer of organic

794 carbon to the deep ocean. Limnol. Oceanogr., 25, 1684-1690, 2001.

795

796 **Dittmar, T., Cherrier, J., and Ludwichowski, K.-U.: The Analysis of Amino Acids in**

797 **Seawater. In: Practical Guidelines for the Analysis of Seawater, CRC Press, 2009.**

798

799 Ebersbach, F., Assmy, P., Martin, P. et al.: Particle flux characterisation and sedimentation

800 patterns of protistan plankton during the iron fertilisation experiment LOHAFEX in the

801 Southern Ocean. Deep Sea Res. I, 89, 94-103, 2014.

802

28

804 Engel, A.: The role of transparent exopolymer particles (TEP) in the increase in apparent

805 particle stickiness (alpha) during the decline of a diatom bloom. J. Plankton Res., 22, 485-

806 497, 2000.

807

808 **Engel, A.: Distribution of transparent exopolymer particles (TEP) in the northeast**

809 **Atlantic Ocean and their potential significance for aggregation processes Deep Sea Res.**

810 **I: Oceanographic Research Papers, 51, 1, 83-92, 2004,**

811

812 Engel, A., Thoms, S., Riebesell, U., Rochelle-Newall, E. and Zondervan, I.: Polysaccharide

813 aggregation as a potential sink of marine dissolved organic carbon. Nature, 428, 929-932,

814 2004.

815

816 Engel, A., Abramson, L., Szlosek, J., Liu, Z., Stewart, G., Hirschberg, D. and Lee, C.:

817 Investigating the effect of ballasting by $CaCO_3$ in *Emiliania huxleyi*, II: Decomposition of

818 particulate organic matter. Deep-Sea Res. II, 56, 18, 1408-1419. DOI

819 10.1016/j.dsr2.2008.11.028, 2009.

820

821 Engel, A.: Determination of Marine Gel Particles, in: Practical Guidelines for the Analysis of

822 Seawater, edited, CRC Press, 2009.

823

824 Engel, A., Piontek, J., Grossart, H. P., Riebesell, U., Schulz, K. G. and Sperling, M.: Impact

825 of CO_2 enrichment on organic matter dynamics during nutrient induced coastal phytoplankton

826 blooms. J Plankton Res., 36, 3, 641-657. DOI 10.1093/plankt/fbt125, 2014.

827

Formatiert: Absatz-Standardschriftart, Schriftart: Times New Roman

Formatiert: Schriftart: Times New Roman, Nicht Kursiv

Gelöscht: Engel, A. und Passow, U.: **Carbon and nitrogen content of transparent exopolymer particles (TEP) in relation to their Alcian Blue adsorption**. Mar. **Ecol. Prog. Ser., 219, 1-10, doi:10.3354/meps219001**, 2001.¶
¶

Formatiert: Schriftart: Nicht Kursiv

Formatiert: Schriftart: Nicht Kursiv

Formatiert: Schriftart: Nicht Kursiv

836 Giering, S. L. C., Sanders, R., Lampitt, R. S.,, Anderson, T. A.,Tamburini, C., Boutrif, M.,

837 Zubkov, M. V., Marsay, C. M., Henson, S. A., Saw, K., Cook, K., and Mayor, D. J.

838 Reconciliation of the carbon budget in the ocean's twilight zone. Nature, 507, 480-483, 2014.

839

840 Haake, B., Ittekkot, V., Ramaswamy, V., Nair, R. R., and Honjo, S. Fluxes of amino acids

841 and hexosamines to the deep Arabian Sea, Mar. Chem., 40, 291–314, 1992.

842

843 Hansen, H.P, and Koroleff, F.: Determination of nutrients. In: Methods of seawater analysis.

844 Grasshof, K. (ed), 159–228, 1999.

845

846 Hecky, R.E., Mopper, K., Kilham, P., and Degens, E. T.: Amino acid and sugar composition

847 of diatom cell-walls. Mar. Biol., 19, 4, 323-331, doi: 10.1007/BF00348902, 1973.

848

849 Heinze, C., Meyer, S.,; Goris, N., Anderson, L., Steinfeldt, R., Chang, N., Le Quere, C., and

850 Bakker, D. C. E. : The ocean carbon sink - impacts, vulnerabilities and challenges. Earth Syst.

851 Dynamics, 6, 1, 327-358, doi: 10.5194/esd-6-327-2015, 2015.

852

853 Iversen, M. H., Nowald, N., Ploug, H., Jackson, G. A., and Fischer, G.: High resolution

854 profiles of vertical particulate organic matter export off Cape Blanc, Mauritania: Degradation

855 processes and ballasting effects. Deep-Sea Res., 57, 6, 771-784,

856 doi:10.1016/j.dsr.2010.03.007, 2010.

857

858 Keil, R. G., Neibauer, J., Biladeau, C., van der Elst, K. and Devol A. H.: A multiproxy

859 approach to understanding the "enhanced" flux of organic matter through the oxygen deficient

860 waters of the Arabian Sea. Biogeosciences, 13, 2077-2092, 2016.

861

872 Klaas, C., and Archer, D. E.: Association of sinking organic matter with various types of

873 mineral ballast in the deep sea: Implications for the rain ratio. Global Biogeochem. Cycles,

874 16(4), 1116, doi:10.1029/2001GB001765, 2002.

875

876 Knauer, G.A., J.H. Martin, and Bruland, K.W.: Fluxes of particulate carbon, nitrogen, and

877 phosphorus in the upper water column of the northeast Pacific. Deep-Sea Research, 26, 97-

878 108, 1979.

879

880 Kohlfeld, K. E., and Ridgewell, A. Glacial-Interglacial Variability in Atmospheric CO2. In:

881 Surface Ocean–Lower Atmosphere Processes Geophysical Research Series, 187, American

882 Geophysical Union, doi:10.1029/2008GM000845, 2009.

883

884 Kwon, E. Y., Primeau, F., and Sarmiento J. L.: The impact of remineralization on the air-sea

885 carbon balance, Nat. Geosci., 2, doi:10.1038/ngeo612, 2009.

886

887 Lam, P. J, Doney, S. C. and Bishop J. K. B.: The dynamic ocean biological pump: Insights

888 from a global compilation of particulate organic carbon, $CaCO_3$ and opal concentrations

889 profiles from the mesopelagic. Global Biogeochem. Cycles., 25, GB3009, doi:

890 10.1029/2010GB003868, 2011.

891

892 Lampitt, R. S., Noji, T. and Von Bodungen, B.: What happens to zooplankton fecal pellets-

893 implications for material flux. Mar. Biol., 104, 1, 15-23, doi: 10.1007/BF01313152, 1990.

894

895 **Le Moigne F., Sanders,** R., **Villa,** M., **Martin,** A., **Pabortsava,** K., **Planquette,** H.,

896 **Morris,** P. J. and **Thomalla**, S.**, On the proportion of ballast vs non-ballast associated**

sinking POC in the surface ocean. Geophys. Res. Letter. doi:10.1029/2012GL052980, 2012.

Lee, C., and Cronin, C.: The vertical flux of particulate nitrogen in the sea: Decomposition of amino acids in the Peru upwelling area and the equatorial Atlantic. J. Mar. Res. 40, 227-251, 1982.

Lee, C., and Cronin, C., Particulate amino acids in the sea: Effects of primary productivity and biological decomposition. Journal of Marine Research 42, 1075-1097, 1984.

Lindroth, P., and Mopper, K.: High performance liquid chromatographic determination of subpicomole amounts of amino acids by precolumn fluorescence derivatization with o-phthaldialdehyde, Analytical Chemistry, 51(11), 1667-1674, 1979.

Löscher, C., Bange, H. W., Schmitz, R. A., Callbeck, C. M., Engel, A., Hauss, H., Kanzow, T., Kiko, R., Lavik, G., Loginova, A. N., Melzner, F., Meyer, J., Neulinger, S. C., Pahlow, M., Riebesell, U., Schunck, H., Thomsen, S. and Wagner, H.: Water column biogeochemistry of oxygen minimum zones in the eastern tropical North Atlantic and eastern tropical South Pacific Oceans. Biogeosciences (BG), 13 . pp. 3585-3606. DOI 10.5194/bg-13-3585-2016, 2016.

Mari, X.: Carbon content and C:N ratio of transparent exopolymeric particles (TEP) produced by bubbling exudates of diatoms. Mar. Ecol. Progr. Ser., 183, 59-71, 1999.

Formatiert: Schriftartfarbe: Schwarz, Englisch (USA)

Gelöscht: Le Moigne, F. A. C., Henson, S. A., Cavan, E., Georges, C., Pabortsava, K., Achterberg, E.P., Ceballos-Romero, E., Zubkov, M. and Sanders, R. J.: What causes the inverse relationship between primary production and export efficiency in the Southern Ocean?, Geophys. Res. Lett., doi:10.1002/2016GL068480, 2016.¶

930 Marsay, C. M., Sanders, R. J., Henson, S. S., Pabortsava, K., Achterberg, E. P., and Lampitt,

931 R. S.: Attenuation of sinking particulate organic carbon flux through the mesopelagic ocean.

932 Proc. Natl. Acad. Sci. U.S.A., 112, 4, 1089-1094, doi: 10.1073/ pnas.1415311112, 2015.

933

934 Martin, P., Lampitt, R. S., Perry, M. J. Sanders, R. Lee, C., and D'Asaro, E.: Export and

935 mesopelagic particle flux during a North Atlantic spring diatom bloom. Deep-Sea Research I

936 58, 338–349, 2011.

937

938 Martin, J.H., G.A. Knauer, D.M. Karl and Broenkow W.W.: Vertex – Carbon Cycling in the

939 Northeast Pacific. Deep-Sea Res. A, 34, 267-285, doi: 10.1016/0198-0149(87)90086-0, 1987.

940

941 Mortlock, R.A., and Froelich, P.N.: A simple method for the rapid determina- tion of biogenic

942 opal in pelagic marine sediments. Deep-Sea Res., Part A, 36, 1415– 1426, 1989.

943

944 Pantoja, S., Sepúlveda, J. and González H. E.: Decomposition of sinking proteinaceous

945 material during fall in the oxygen minimum zone off northern Chile. Deep Sea Research, I,

946 51, 55-70, 2004.

947

948 Passow, U.: Transparent exopolymer particles (TEP) in aquatic environments, Progress in

949 Oceanography, 55, 287-333, 2002.

950

951 Passow, U., Shipe, R. F., Pak, D. K., Brzezinski, M. A., & Alldredge, A. L.: Origin of

952 transparent exopolymer particles (TEP) and their role in the sedimentation of particulate

953 matter. Continental Shelf Research, 21, 327–346, 2000.

954

955 Ploug, H., Kühl M., Buchholz-Cleven, B., and Jørgensen, B.B.: Anoxic aggregates - an

956 ephemeral phenomenon in the pelagic environment? Aquat. Microb. Ecol., 13, 285–294,

957 1997.

958

959 Ploug, H., and Bergkvist, J.: Oxygen diffusion limitation and ammonium production within

960 sinking diatom aggregates under hypoxic and anoxic conditions. Mar. Chem. 176, 142-149,

961 2015.

962

963 Schlitzer, R., Ocean Data View, http://odv.awi.de, 2013.

964

965 Schneider, B., Engel, A., and Schlitzer, R.: Effects of depth- and CO2-dependent C:N ratios

966 of particulate organic matter (POM) on the marine carbon cycle. Global Biogeochemical

967 Cycles, 18, 2, doi:10.1029/2003GB002184, 2004.

968

969 Soutar, A., Kling, S. A., Crill, P. A., Duffrin, E., and Bruland K.W.: Monitoring the marine

970 environment through sedimentation. *Nature*, 266, 136-139, 1977.

971

972 Stief, P., Kamp, A., Thamdrup, B., and Glud, R.N. : Anaerobic Nitrogen Turnover by Sinking

973 Diatom Aggregates at Varying Ambient Oxygen Levels. Frontiers in Micriobiol., 7, 98 doi:

974 10.3389/fmicb.2016.00098, 2016.

975

976 Stramma, L., Johnson, G. C., Sprintall, J., and Mohrholz, V.: Expanding Oxygen-Minimum

977 Zones in the Tropical Oceans, Science, 320, 655-658, 2008.

978

979 Suess, E.: Particulate organic carbon flux in the oceans - surface productivity and oxygen

980 utilization, Nature 288, 260–263, 1980.

Gelöscht: ¶
Ploug, H., and B.B. Jørgensen (1999) A net-jet flow system for mass transfer and microelectrode studies in sinking aggregates. Mar. Ecol. Prog. Ser. 176, 279-290. ¶

987

988   Torres Valdez, S., Painter, . C., Martin, A. P., Sanders, R. and Felden, J.: Data compilation of

989   fluxes of sedimenting material from sediment traps in the Atlantic Ocean. Earth system

990   Science Data, 6, 123-145, doi: 10.5194/essd-6-123-2014, 2014.

991

992   Van Mooy, B. A. S., Keil R. G., and Devol, A. H.: Impact of suboxia on sinking particulate

993   organic carbon: Enhanced carbon flux and preferential degradation of amino acids via

994   denitrification. Geochim. Cosmochim. Ac., 66, 457-465. doi: 10.1016/s0016-7037(01)00787,

995   2002.

996

997   Visbeck M.: Oxygen in the Tropical Atlantic OSTRE Second Tracer Survey – Cruise. No.

998   M105 – March 17 – April 16, 2014 – Mindelo (Cape Verde) – Mindelo (Cape Verde).

999   METEORBerichte, M105, 49 pp., DFG-Senatskommission für Ozeanographie,

1000 DOI:10.2312/cr_m105, 2014.

1001

1002 Volk, T., and Hoffert, M. I.: Ocean carbon pumps: Analysis of relative strengths and

1003 efficiencies in ocean driven atmospheric CO2 changes. In: Sundquist ET and Broecker WS

1004 (eds.) The Carbon Cycle and Atmospheric CO2: Natural Variations Archean to Present,

1005 Geophysical Monograph Series, vol. 32, pp. 99-110. Washington, DC: American Geophysical

1006 Union, 1985.

1007

1008 Weiner, S. and Erez, J.: Organic matrix of the shell of the foraminifer *Heterostegina*

1009 *depressa*. Journal of Foraminifera Res., 14, 3, 206-212, 1984.

1010

1011 Welschmeyer, N. A.: Fluometric analysis of chlorophyll a in the resence of chlorophyll b and

1012 pheopigments. Limnol. Oceanogr., 39, 1985-1992, 1994.

Tables

Table 1: Fluxes of particulate components at 100m depth (F_{100}) and in the core of the OMZ at 400m (F_{OMZ}), as well as the associated attenuation coefficients (*b*-values) and transfer efficiencies (T_{eff}, %) over the depth range 100 to 600 m during two traps deployments in the ETNA. All units are in mg m^{-2} d^{-1} except for TEP fluxes which is reported in total particle area cm^{-2} m^{-2} d^{-1}. Mean values and standard deviations (SD) were calculated from analytical replicates.

Component		F_{100}		F_{OMZ}		*b*-value			T_{eff} (%)
		mean	SD	mean	SD	mean	SD	r²	(600/100 m)
Mass	I	249	48.9	141	6.8	-0.429	0.090	0.987	41
	II	231	16.3	141	12.1	-0.355	0.033	0.998	52
POC	I	69.4	9.23	23.8	5.4	-0.795	0.031	0.989	23
	II	76.3	8.43	28.1	3.0	-0.741	0.044	0.989	22
PN	I	11.9	1.29	2.76	0.46	-1.013	0.026	0.992	15
	II	13.5	1.12	3.26	0.19	-1.00	0.020	0.990	16
POP	I	0.71	0.07	0.15	0.02	-1.081	0.074	0.992	18
	II	0.64	0.03	0.22	0.02	-0.80	0.034	0.990	23
Opal	I	44.6	1.76	34.0	1.7	-.0195	0.038	0.987	65
	II	48.6	4.16	30.7	2.0	-0.345	0.052	0.987	44
Chl *a*	I	0.10	0.00	0.035	0.001	-0.820	0.024	0.990	21
	II	0.12	0.01	0.053	0.005	-0.625	0.082	0.988	24
TEP	I	1650	548	119	36.8	-0.498	0.014	0.548	33
	II	2990	348	1644	95	-0.451	0.069	0.810	37
PHAA-C	I	3.21	-	3.71	0.47	-1.324	0.067	0.994	11
	II	1.28	0.10	5.24	0.79	-0.978	0.096	0.991	14

1026 Table 2: Composition (%Mol) and degradation index (DI) of PHAA collected at different depths during two trap deployments (#I, #II) in the ETNA
1027 region.

Depth(m)	AsX	GlX	Ser	Gly	Thr	Arg	Ala	GABA	Tyr	Val	Iso	Phe	Leu	DI
#I														
60	14.15	13.94	8.46	14.29	7.76	5.90	11.94	0.22	0.84	5.69	4.57	4.00	8.26	0.34
100	13.95	13.53	8.29	14.65	7.87	5.77	11.57	0.19	1.64	5.66	4.56	4.07	8.24	0.23
150	14.19	12.73	8.54	15.93	8.10	5.78	11.42	0.31	0.96	5.68	4.44	4.05	7.87	0.29
200	14.17	12.05	9.29	16.02	8.05	5.61	11.69	0.49	1.10	5.65	4.30	4.04	7.54	0.07
300	13.19	11.75	8.58	17.71	7.98	5.31	12.10	0.37	1.82	5.77	4.15	3.83	7.43	0.03
400	14.15	11.77	9.03	18.54	7.94	5.72	10.85	0.46	1.25	5.58	3.93	3.80	6.97	0.02
500	14.06	11.89	9.55	18.70	7.18	6.01	11.02	0.55	1.29	5.19	3.86	3.65	7.05	0.02
600	14.15	13.94	8.46	14.29	7.76	5.90	11.94	0.22	0.84	5.69	4.57	4.00	8.26	0.07
#II														
100	13.89	14.69	8.36	12.94	7.57	5.89	12.26	0.21	0.02	6.13	5.12	4.05	8.86	0.24
150	13.48	14.23	8.46	14.12	7.56	5.68	12.55	0.22	0.00	6.21	5.01	3.85	8.62	0.37
200	13.80	13.90	9.10	14.27	7.20	6.12	11.57	0.27	0.04	6.19	5.07	3.97	8.49	0.13
300	14.58	14.63	8.35	15.16	7.75	5.56	11.75	0.26	0.14	5.62	4.51	3.82	7.88	0.07
400	14.06	13.01	8.72	16.45	7.99	5.55	11.74	0.44	0.79	5.54	4.33	3.77	7.59	0.08
500	14.08	12.90	8.75	16.48	7.59	5.69	11.81	0.37	0.30	5.94	4.62	3.80	7.66	-0.09

| 600 | 13.62 | 12.55 | 9.16 | 17.02 | 7.95 | 5.75 | 11.23 | 0.42 | 0.38 | 5.87 | 4.61 | 3.88 | 7.55 | -0.04 |

1029 **Figure captions:**
1030
1031
1032 Figure 1a-d: Map of the study area (A) and depth distribution of oxygen concentration (mol

1033 kg^{-1}) (B) in the Eastern Tropical North Atlantic (ETNA) during the RV Meteor 105 cruise,

1034 when two surface tethered drifting sediment traps (STDT) were deployed (C). Depth

1035 distribution of oxygen concentration (mol kg^{-1}) at stations visited in the deployment area

1036 showed an oxygen minimum zone in the upper mesopelagial (D).

1037

1038 Figure 2a-d: Fluxes of total mass (a) and particulate organic carbon (b; POC), particulate

1039 nitrogen (c; PN), and particulate organic phosphorus (d; POP) during the deployment of two

1040 STDT in the ETNA. Deployments: Solid symbols #I, open symbols #II.

1041

1042 Figure 3a-d: Fluxes of Chlorophyll *a* (a; Chl *a*), opal (b), TEP (c), and PHAA (d) during the

1043 deployment of two STDT in the ETNA. Deployments: Solid symbols #I, open symbols #II.

1044

1045 Figure 4: Changes in mineral ballast ratios of sinking particles with depth during the two

1046 deployments in the ETNA. Deployments: Black bars #I, grey bars #II.

1047

1048 Figure 5a-f: Changes in organic matter composition of particles sinking through the OMZ

1049 during the deployment of two STDT in the ETNA. Deployments: Solid symbols #I, open

1050 symbols #II.

1051

1052 Figure 6a-d: Molar percentages of selected amino acids contained in PHAA during the

1053 deployment of two STDT in the ETNA. Deployments: Solid symbols #I, open symbols #II.

1054

1055   Figure 7: Degradation index (DI) of organic matter in trap collected sinking particles based on

1056   amino acid composition and calculated after Dauwe et al. (1999). Deployments: Black bars
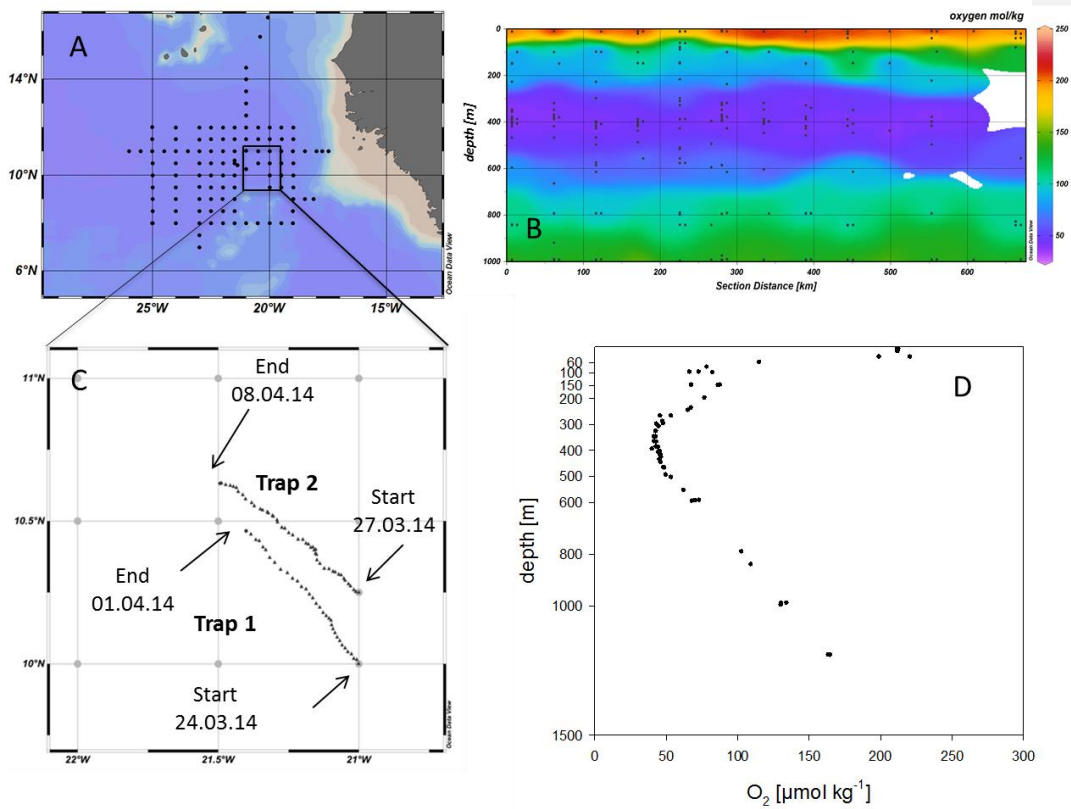
1057   #I, grey bars #II.

1058

1059

1060

Figures

1065

1066

1067

1068

1069

Figure 1a-d
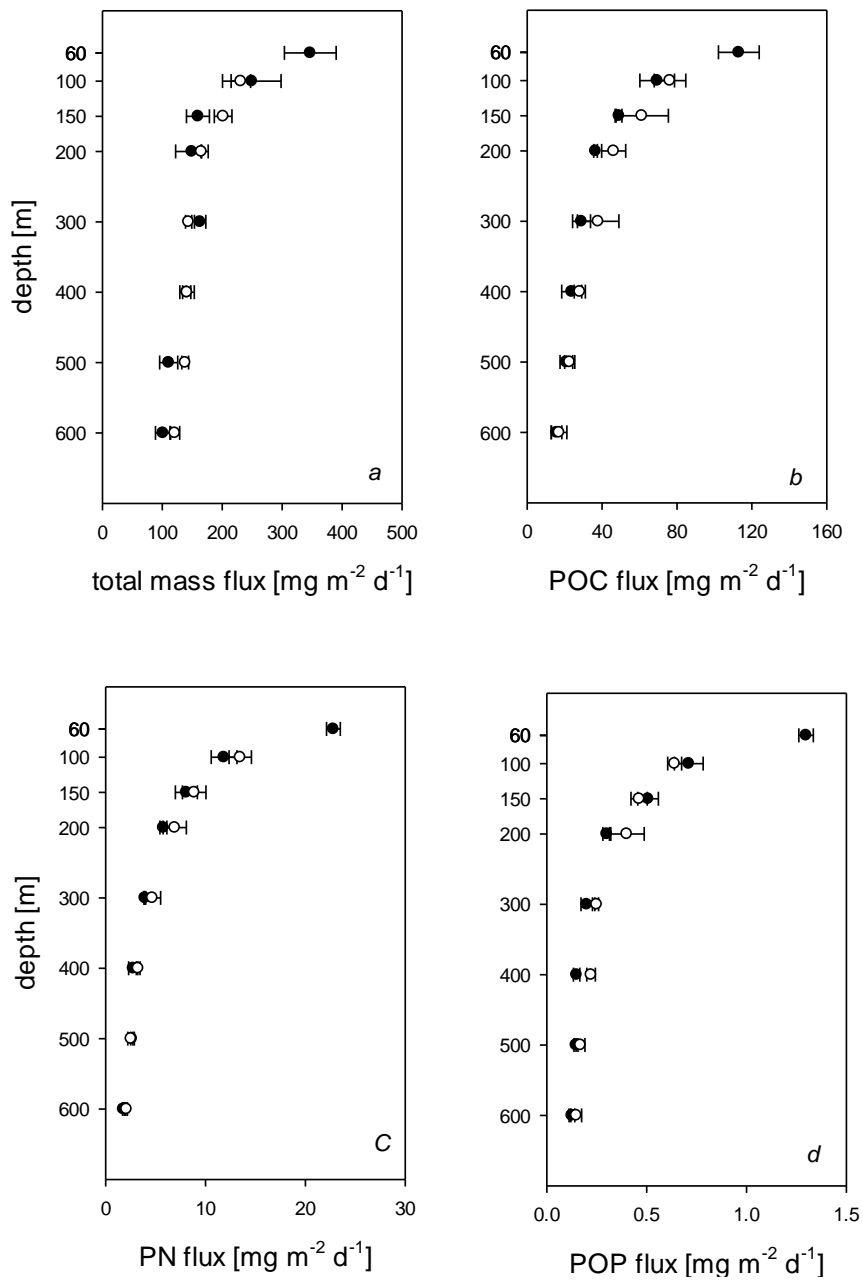
1071

Figure 2a-d

Figure 3a-d

1099

1100

1101

1102
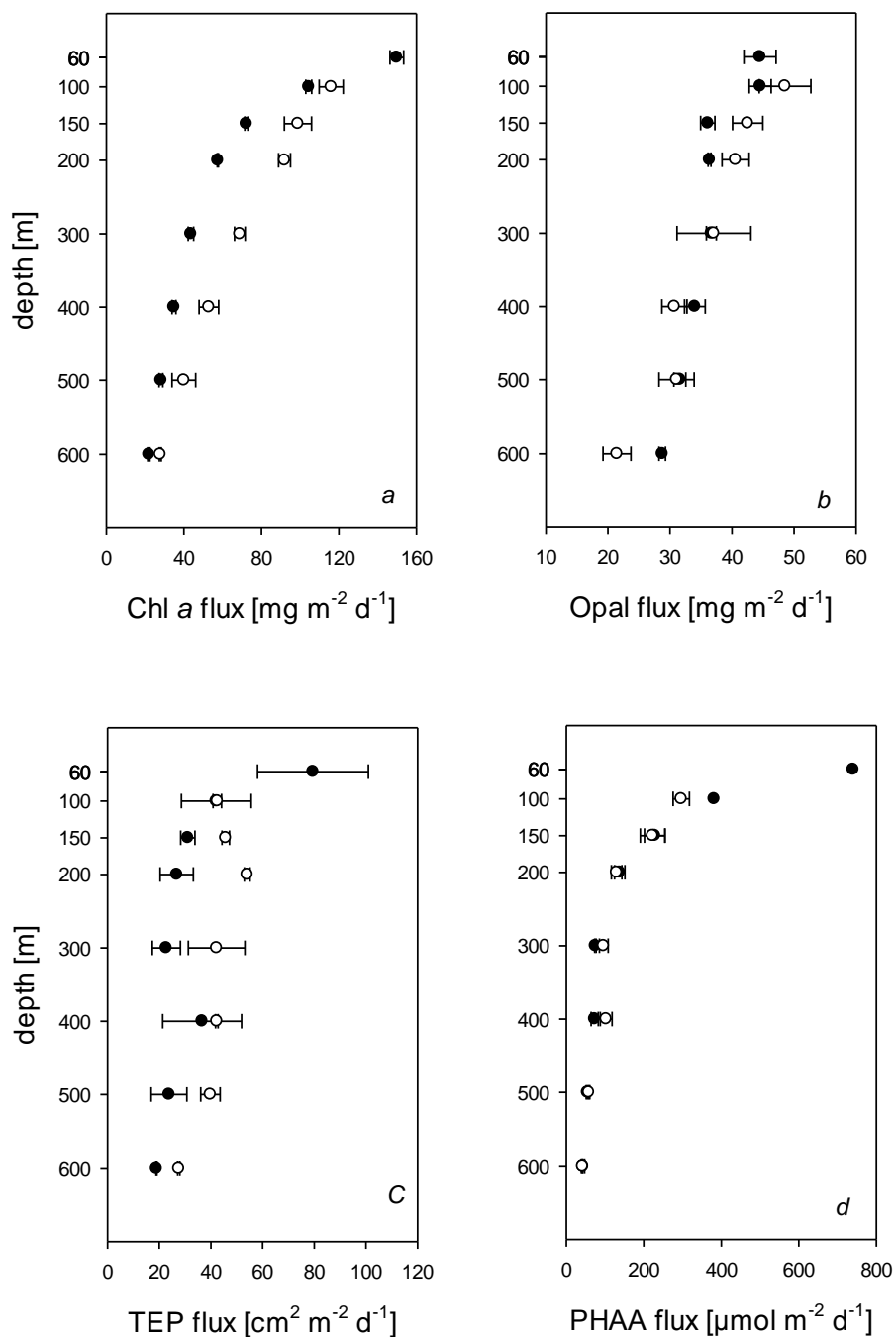
1103

1104

1105

1106

1107

1108

1109

1110

1111

1112
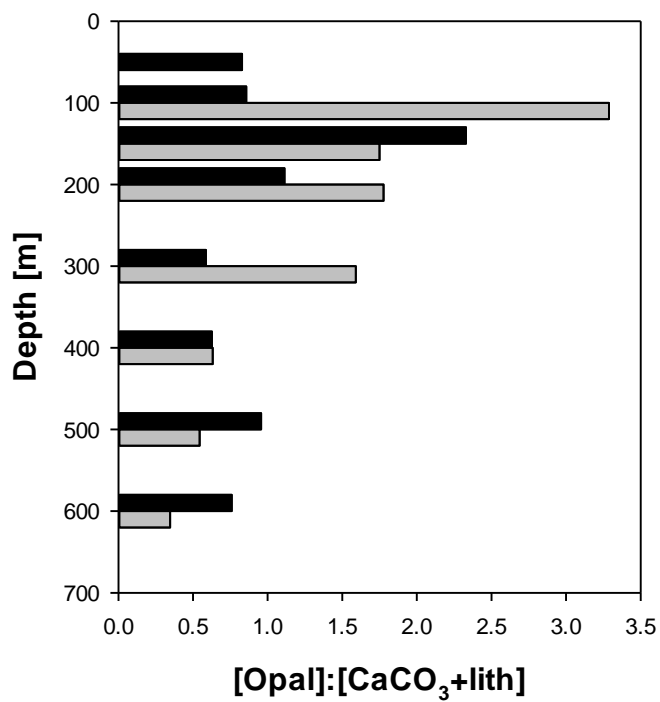
1113

1114

1115

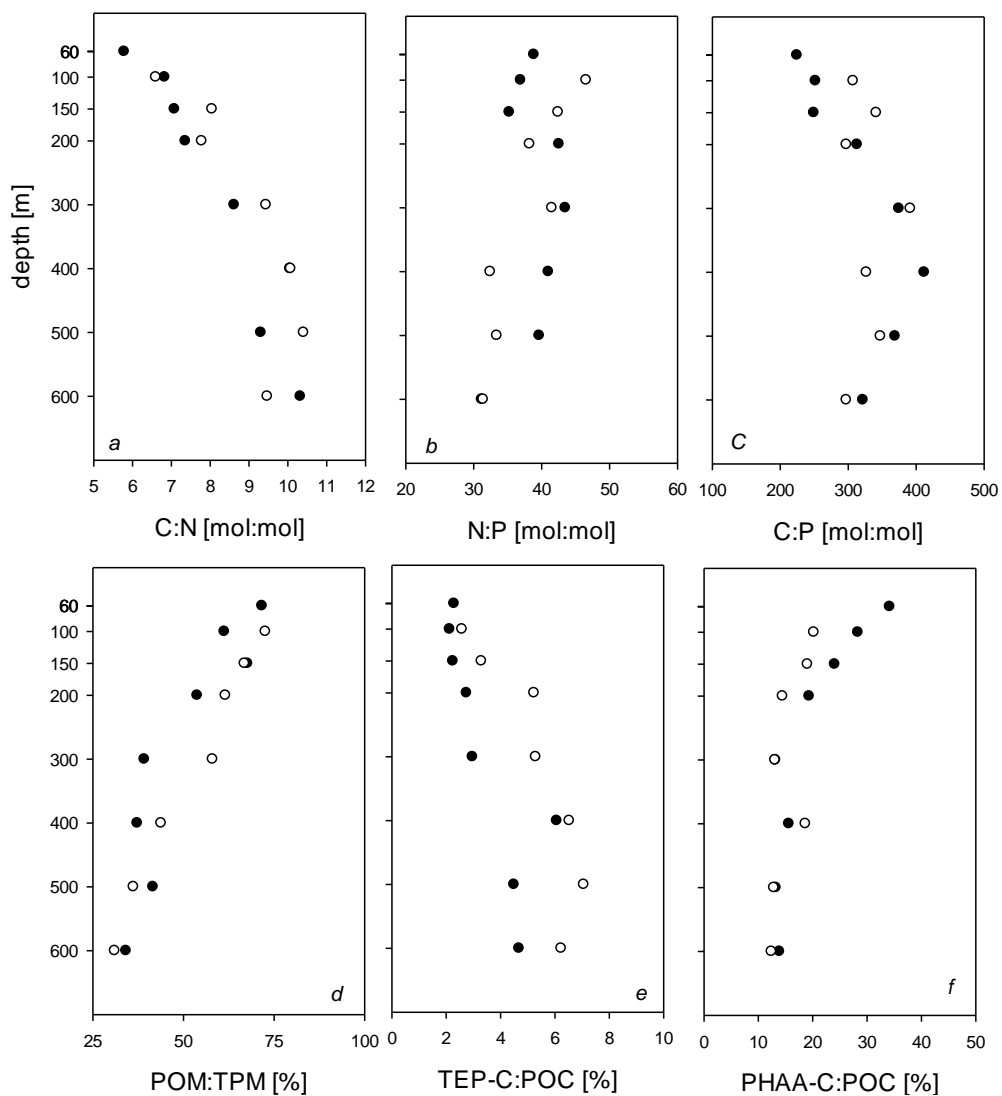1116

1117

1118

1119

1120

1121

1122

Figure 4

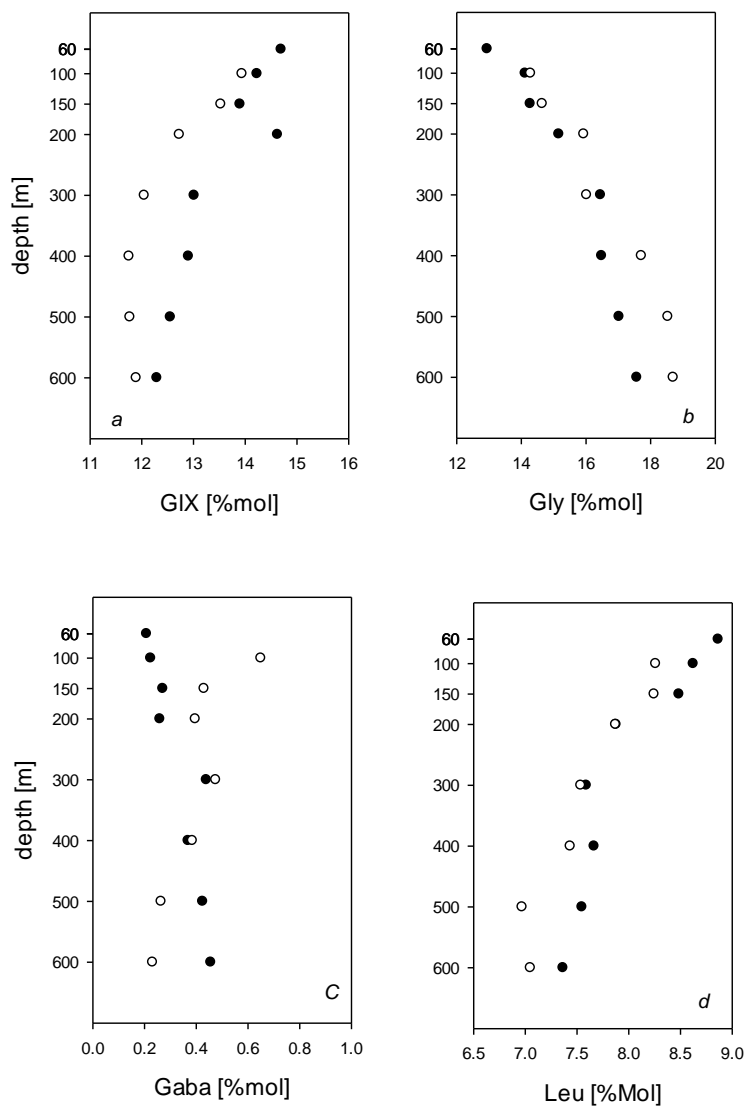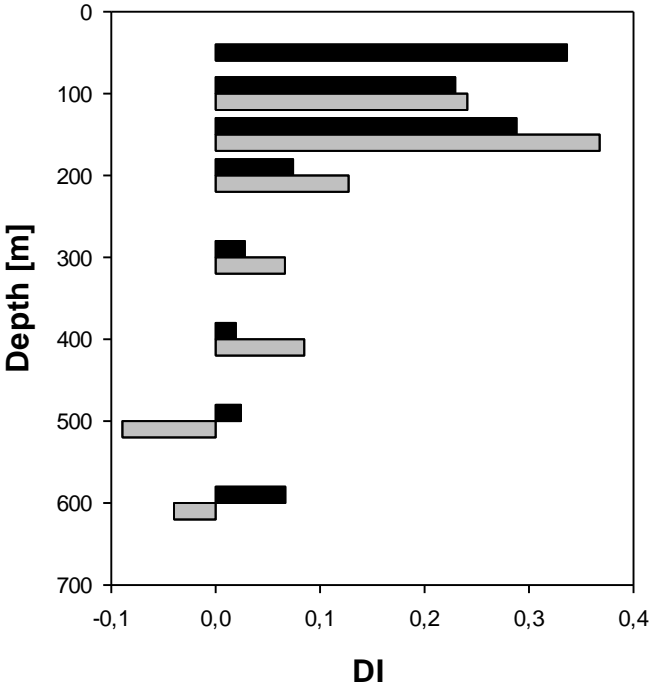1123

1124

1125   Figure 5a-f

1126

1127

1128

1129

1130

1131

1132

1133

1134   Figure 6a-d

1135

1136

1137

1138

1141

1142

1143   Figure 7